

## Climate change and wildfire in California

A. L. Westerling · B. P. Bryant

Received: 2 August 2006 / Accepted: 5 October 2007 / Published online: 12 December 2007  
© Springer Science + Business Media B.V. 2007

**Abstract** Wildfire risks for California under four climatic change scenarios were statistically modeled as functions of climate, hydrology, and topography. Wildfire risks for the GFDL and PCM global climate models and the A2 and B1 emissions scenarios were compared for 2005–2034, 2035–2064, and 2070–2099 against a modeled 1961–1990 reference period in California and neighboring states. Outcomes for the GFDL model runs, which exhibit higher temperatures than the PCM model runs, diverged sharply for different kinds of fire regimes, with increased temperatures promoting greater large fire frequency in wetter, forested areas, via the effects of warmer temperatures on fuel flammability. At the same time, reduced moisture availability due to lower precipitation and higher temperatures led to reduced fire risks in some locations where fuel flammability may be less important than the availability of fine fuels. Property damages due to wildfires were also modeled using the 2000 U.S. Census to describe the location and density of residential structures. In this analysis the largest changes in property damages under the climate change scenarios occurred in wildland/urban interfaces proximate to major metropolitan areas in coastal southern California, the Bay Area, and in the Sierra foothills northeast of Sacramento.

### 1 Introduction

Wildfire activity in California and the western U.S. has greatly increased in recent years (Westerling et al. 2006), as has its economic impact (NOAA 2005). This increase has been particularly acute in western forests, including those of the Sierra Nevada, Southern Cascade, and Coast Ranges of northern California (Westerling et al. 2006), while trends in western wildfire activity in non-forest vegetation types are less readily apparent in the available documentary wildfire histories (Westerling et al., in preparation).

Westerling et al. (2006) attribute the increase in western U.S. forest wildfires to warmer spring and summer temperatures, reduced precipitation associated with warmer temper-

---

A. L. Westerling (✉)  
University of California, Merced, CA, USA  
e-mail: awesterling@ucmerced.edu

B. P. Bryant  
Pardee RAND Graduate School, Santa Monica, USA

atures, reduced snowpack and earlier spring snowmelts, and longer, drier summer fire seasons in some middle and upper elevation forests. These are trends that are projected to continue under plausible climate change scenarios (National Assessment Synthesis Team 2000, Houghton et al. 2001, Running 2006), implying a further increase in the risk of large, damaging forest wildfires in parts of California and the region.

In contrast, future grass and shrubland wildfire risks under climate change scenarios are less clear. Active wildfire years in these ecosystems tend to be strongly associated with positive growing season moisture anomalies a year or more prior to the fire season, and less influenced by moisture anomalies concurrent with the fire season itself (Westerling et al. 2003a), consistent with fire regimes where moisture available to promote the growth and carry-over of fine fuels (grasses, forbs, etc.) is a limiting factor. Precipitation tends to be somewhat more variable than temperature across global climate models and scenarios, implying greater uncertainty for non-forest wildfire risks, while warmer temperatures might tend to reduce the moisture available to plants during the growing season.

Wildfire risks and their economic impacts already pose a significant management challenge to local, state and federal authorities in California, which together spend over \$1 billion per year on fire suppression (California Board of Forestry 1995). This challenge is likely to increase with climate change and continued growth in the state. California's wildland-urban interface, where property values are most directly at risk to losses due to wildfires, encompasses more than 5 million homes (Stewart et al. 2006), making wildfire a particularly important source of potential climate change impacts for the state.

In this analysis, we sought to develop an analytical framework and modeling approach to begin quantifying how wildfire risks and property losses due to those risks will change under different climate scenarios. We developed a logistic probability model to estimate the probability of fires exceeding a threshold of 200 ha (approximately 500 acres) occurring in any given month as functions of climate, hydrology, and topography. This model was estimated using observed 1980–1999 large fire frequency, precipitation, temperature, simulated hydrologic variables (soil moisture, snow) and elevation as a baseline. The 1980–1999 period was used because this is the longest period for which all of these data were available. We then used this model to investigate how large fire risks could change under four scenarios for future climate. Wildfire risks for the GFDL and PCM global climate models and the A2 and B1 emissions scenarios were compared for 2005–2034, 2035–2064, and 2070–2099 against a modeled 1961–1990 reference period in California and neighboring states. The climate change scenarios examined here (see Cayan et al., this issue) ranged from a scenario with increased precipitation and temperatures increasing less than 2°C (PCM B1), to a scenario with decreased precipitation and temperatures increasing more than 4°C (GFDL A2).

Change in the frequency of fires greater than 200 ha is not the only metric by which climate change impacts on wildfire could be assessed. Changes in total burned area or in the severity of fires' ecological or economic impacts are also pertinent. While we do consider some economic impacts here, a comprehensive assessment of the total impact of climate change on wildfire is beyond the scope of this work. However, we suspect that changes in total burned area and the severity of ecological and other economic impacts would tend to be positively correlated with changes in large wildfire frequency.

To estimate the economic damage caused by wildfires, we associated spatial property data with the geographic location of past and hypothetical wildfires to estimate the expected number of structures at risk, structures lost, and the value of these structures, for wildfires 200 ha in size in California. Since our logistic probability model estimated the risk of fires equal to or greater than 200 ha in size, the damages reported here are our best currently

available estimate of the expected minimum impact of wildfire on property for the four climate change scenarios considered here. It is important to keep in mind as well that these damages represent just one dimension of the economic impact of wildfire. Fire suppression and prevention expenditures, health effects of fire-caused pollution, effects on subsequent runoff, flooding, erosion and water quality, altered recreation opportunities, loss of forest and range resources, habitat changes, and altered passive uses (e.g., viewsheds) all have their own costs and benefits that reflect economic impacts of wildfire.

While this work focuses on California and parts of neighboring states, the methodologies described here are generally applicable to modeling wildfire risks and related property losses under climate change scenarios.

## 2 Climate and wildfire in California

Climate affects wildfire risks primarily through its effects on moisture availability. Wet conditions during the growing season promote fuel – especially fine fuel (grasses, etc.) – production via the growth of vegetation, while dry conditions during and prior to the fire season increase the flammability of the live and dead vegetation that fuels wildfires. Moisture availability is a function of both cumulative precipitation and temperature. Warmer temperatures can reduce moisture availability via an increased potential for evapotranspiration, a reduced snowpack (e.g., more rain and less snow), and an earlier snowmelt. In California, 95% of annual water-year (i.e., October to September) precipitation occurs by the end of May (Westerling et al. 2003b). Snowpack at higher elevations is an important means of making part of winter precipitation available as runoff in late spring and early summer (Sheffield et al. 2004), and a reduced snowpack and earlier snowmelt consequently lead to a longer, drier summer fire season in many mountain forests (Westerling et al. 2006).

The relative importance of fuel availability vs flammability for wildfire risks varies with the type of vegetation. At one extreme, a relatively wet, densely forested ecosystem will have abundant fuel, so that the incremental effect of a single wet season on fuel availability will be negligible, and vegetation is buffered to some extent from the effects of temperature by moisture reservoirs in snow and soils. In such an ecosystem, fuel flammability is usually the limiting factor for wildfire risks. For convenience, we will refer to systems like this as energy-limited fire regimes: large fires can occur when there is sufficient energy available to dry out the plentiful fuels (see e.g., Balling et al. 1992, Swetnam and Betancourt 1998, Donnegan et al. 2001, Westerling et al. 2002 and 2003a, Heyerdahl et al. 2002).

At the opposite extreme, in a relatively dry ecosystem dominated by grass and low-density shrub vegetation types, fuel coverage may be so sparse that in some years the spread of large fires is limited by fuel availability. When such an ecosystem receives above-normal precipitation, fire risks may be subsequently elevated for a time, as excess moisture leads to the growth of additional vegetation that quickly dries out in the typically dry summer months and provides more continuous fuel coverage.<sup>1</sup> We will refer to these systems as moisture-limited fire regimes: large fires can occur when antecedent moisture results in an increased fuel load (Westerling et al. 2003a).

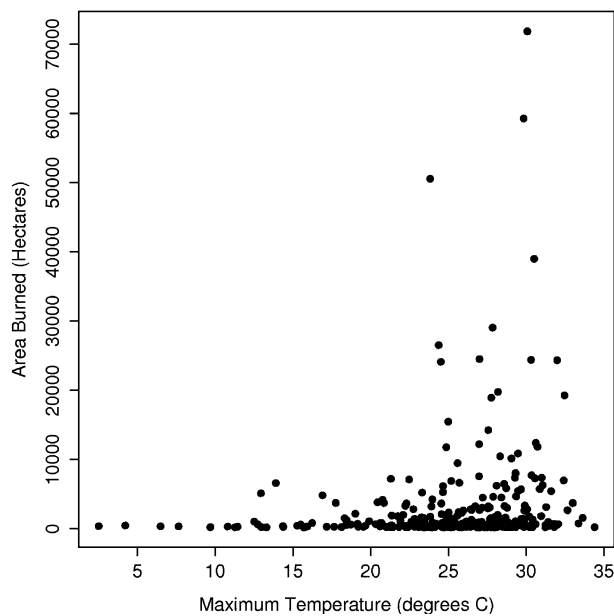
<sup>1</sup> The mechanism for the link between antecedent moisture and subsequent fire risk (i.e. the growth of fine fuels to provide a more continuous fuel coverage) is an hypothesis supported by robust statistical tests using observationally-determined soil moisture and the Palmer Drought Severity Index but has not been conclusively documented from *in situ* or satellite observations of fuels themselves.

While these two scenarios are a simplification of two extremes among the great variety of both vegetation and fire regime types found in California, they provide a useful context for understanding statistical relationships between historically observed fire activity and the climatological factors that drive fuel flammability and availability (i.e., precipitation and temperature). For example, Westerling et al. (2003a) found annual area burned in south-eastern California (moisture-limited) deserts was highly correlated with growing season moisture anomalies the preceding year, but not with current year drought. Conversely Swetnam (1993) using paleofire reconstructions and Westerling et al. (2003a) using documentary fire histories found Sierra Nevada forest wildfire activity was significantly associated with current year drought.

The consequence of the risk of forest wildfires being so strongly contingent on summer drought is that these risks tend to be associated with relatively high temperatures (Fig. 1) (Swetnam 1993, Westerling et al. 2006). Over three quarters of the months with one or more fires in excess of 200 ha in locations that we categorized in our model as energy-limited (i.e., 20-year-average soil moisture  $\geq 28\%$  of capacity, see below) occurred when maximum temperatures exceeded 23°C. Likewise, all of the months with total area burned exceeding 10,000 ha in these locations occurred when maximum temperatures exceeded 23°C. A maximum temperature of 23°C or greater was in the 64th percentile of maximum temperatures over the 1980–1999 period for which comprehensive wildfire data were available.

Because moisture surplus or deficit conditions during the fire season itself are not significant indicators of risk for predominantly moisture-limited fire regimes (Westerling et al. 2003a), increases in temperature during the fire season are not likely to have as dramatic an effect on risks for these fires as they could for energy-limited fire regimes. Indirectly, however, changes in temperature may have an effect on moisture-limited wildfire risks through their potential to affect the moisture available for the growth of vegetation during the growing season. For example, warmer temperatures could contribute to a reduction in moisture-limited fire risks if they led to reduced growing season moisture

**Fig. 1** Each point represents the total area burned in one grid cell in 1 month in large wildfires in energy-limited fire regimes of California and neighboring states vs the average monthly maximum temperature for that month and grid cell for the 1980–1999 period



availability and less vegetation. However, effects of any changes in precipitation might be as or more relevant than changes in temperature in this particular case.

### 3 Climate change scenarios

We analyzed potential impacts of four climate change scenarios on wildfire in California (see Cayan et al., this issue). These scenarios corresponded to “business as usual” (A2) and “transition to a low greenhouse gas emissions” (B1) emissions scenarios in two global climate models (Geophysical Fluid Dynamics Laboratory (GFDL) and Parallel Climate Model (PCM)). The A2 high-emissions scenario corresponds to a CO<sub>2</sub> concentration by end of century of more than three times the pre-industrial level, while the B1 low-emissions scenario results in a doubling of pre-industrial CO<sub>2</sub>. In all four scenarios California experienced warmer temperatures, with the greatest increase in the GFDL A2 scenario (averaging a 4.30°C increase for California by 2070–2099 as compared to 2061–2090). These results are consistent with temperatures simulated under a broad array of climate change models. The variability in projected future temperatures across simulations using the same emissions scenarios is indicative of variability in the sensitivity of the modeled climate systems to increased greenhouse gases. It is important to note, however, that virtually all climate models project warmer springs and summers will probably occur over the region in coming decades under plausible future emissions scenarios.

Future changes in precipitation under climate change scenarios are generally less certain than for temperature. This uncertainty is evident in the scenarios discussed here, with the PCM B1 scenario showing increased precipitation over most of the state by 2070–2099, the PCM A2 showing increased precipitation in southern and central California and decreased precipitation in Northern California by 2070–2099, and the GFDL A2 scenario showing decreased precipitation statewide by 2070–2099.

This uncertainty in projected precipitation means that, for regions where variability in fire risks tends to be dominated by variability in precipitation rather than in temperature (i.e., moisture limited fire regimes), projected fire risks may also exhibit similar uncertainty. Conversely, where variability in fire risks is dominated by variability in temperature (i.e., energy-limited fire regimes), projected changes in wildfire risks should show some consistency across climate change models in terms of the direction of change (i.e., increased vs decreased fire risks).

### 4 Data and methods

#### 4.1 Domain of analysis

This analysis covered California, Nevada, and parts of neighboring states on a 1/8° grid contained within 124.5625° to 113.0625° West Longitude and 31.9375° to 43.9375° North Latitude. Fire histories and climatologic and hydrologic explanatory variables were aggregated to a monthly temporal resolution from 1980 to 1999. This yielded 2,165,040 voxels<sup>2</sup> comprising a 93×97 spatial grid for 240 months (93 1/8° of latitude by 97 1/8° of longitude by 240 months).

<sup>2</sup> I.e. “volume pixel,” the smallest component box defined by a three-dimensional grid (where one dimension is in this case time).

The study masked out the Pacific Ocean, some areas converted to agriculture or other uses<sup>3</sup>, and grid cells corresponding to lands managed by agencies for which we had no fire histories (Department of Defense, Bureau of Reclamation, Fisheries and Wildlife Service, and the Department of Energy's Nevada Test Site). Some additional grid points were excluded because we had no hydrologic data simulated for them. The result was a 1,490,160-voxel domain including California and Nevada and parts of Arizona, Utah, Idaho and Oregon.

#### 4.2 Fire history

Fire occurrence data for fires greater than 200 ha for 1980–1999 were compiled from the USDA Forest Service (USFS); from the United States Department of the Interior's (USDI's) Bureau of Land Management (BLM), National Park Service, and Bureau of Indian Affairs (BIA); from the state lands or forestry agencies of Oregon, Utah, Arizona, and California; and from contract counties in California. Fire occurrence data from the State of Nevada's Division of Forestry was not included; however, fire records for the protection responsibility areas of BLM, BIA, and USFS in Nevada still afforded comprehensive coverage of most of the state's wildlands.

These data were assembled as part of an effort to extend the Canadian Large Fire History to Alaska and the western contiguous United States, providing a comprehensive western North American large fire history. The Canadian Large Fire History contains fires that burned at least 200 ha, so that arbitrary threshold was applied to the U.S. data as well. In general, the small fraction of ignitions that become large fires (here a few percent of total ignitions) accounts for most wildfire area burned, damages, and suppression expenditures, and the quality of these large fires' documentary records tends to be much better than for the more numerous very small fires. Limiting analysis to fires above a 200-ha threshold thus yields a relatively comprehensive, higher quality data set where the number of fires included is small enough that quality assurance efforts are feasible (Westerling et al. 2006). There were 3,137 voxels where at least one fire exceeded 200 ha in the sampled period, and 1,487,023 voxels where no fires were observed above this minimum threshold (see Fig. 2 for the spatial extent of the fire record).

#### 4.3 Hydrologic simulation

Historical soil moistures and snow water equivalent were simulated at 1/8° resolution over the entire domain (by Maurer, this issue) with the Variable Infiltration Capacity (VIC) hydrologic model (Liang et al. 1994, 1996) using temperature and precipitation from the gridded National Climatic Center Cooperative Observer station data set (Maurer et al. 2002). The VIC model used here was calibrated to match streamflow records at several points in California and the Northwest. While the streamflow records provide an integrative measure of hydrologic processes in the major drainage basins of the region, the resulting soil moistures were not independently validated against *in situ* measurements. Soil moistures

<sup>3</sup> Grid cells where the sum of the fractional areas classified as “agricultural” and “urban and built-up” by the fractionally adjusted University of Maryland vegetation classification scheme (UMDvf) was greater than the sums for forested categories, for shrubland categories, and for grassland categories, were excluded if no wildfires occurred there during 1980–1999. Highly urbanized areas in the 2000 census classified as grassland in UMDvf where no large wildfires were reported during 1980–1999 were also excluded.

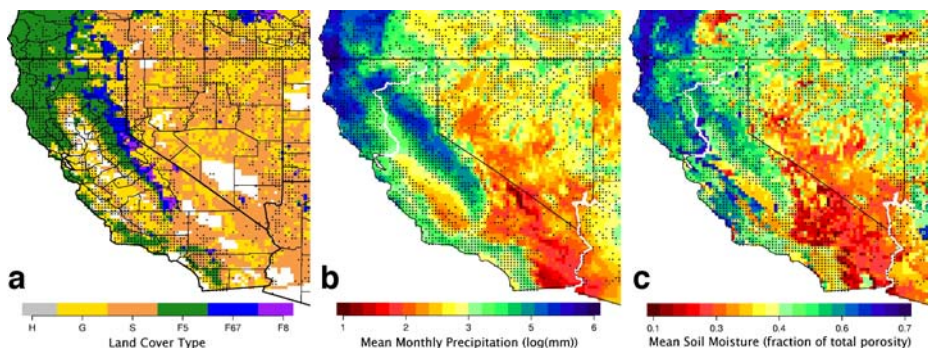


**Fig. 2** There is a strong correspondence between coarse vegetation types, available moisture, and the incidence of large fires. **a** Dominant vegetation type: *H* human – urban and agricultural, *G* grass, *S* shrub, *F5* forest below 5,500 ft elevation, *F67* forest between 5,500 and 7,500 ft elevation, *F8* forest above 7,500 ft. **b** Monthly mean precipitation 1970–1989. **c** VIC modeled soil moisture. *White areas* are masked out (Pacific Ocean, urban and agricultural conversion, and land management agencies not included in our fire history). *Black dots* indicate a grid cell with at least one fire >200 ha (494 acres) in our fire history. All variables are plotted on a 1/8° grid

from un-calibrated VIC runs appear to be more strongly associated with fire risks than were the calibrated soil moistures analyzed here.

#### 4.4 Predictors

Elevation and hydroclimatic indices derived from precipitation, maximum temperature, soil moistures, and snow water equivalent, were examined as potential predictors for large fire risk, along with elevation. For each voxel, a record was created containing the following variables, arranged in order from those that vary on monthly time scales to those that are fixed or nearly fixed over the historical sample. Data from all voxels, pooled together, were used to estimate the model coefficients:

SMI	current soil moisture index from the VIC hydrologic model, estimating soil moisture as percent of total soil porosity
PREC	precipitation for the current month
TMAX	monthly mean of daily maximum temperatures for the current month
TAVG	mean March through August temperature for the current year
SMI12m	maximum SMI over the preceding 12 months
PREC12	cumulative precipitation for the preceding 12 months
PREC12.6	PREC12 leading by 6 months (i.e., cumulative precipitation for the preceding 18 to 7 months)
SMI20	the average monthly SMI over the preceding 20 years
WET	True/False factor, defined as $SMI20 \geq 28\%$
SI	snow index = $1 - SFI/12$ , where SFI is the average number of snow-free months over the preceding 20 years. It is the percent of the year a location has snow cover. Derived from VIC-simulated snow water equivalent.
ELEV	mean elevation derived from GTOPO30 Global 30 Arc Second (approximately 1 km) Elevation Data Set, distributed by the North American Land Data Assimilation System ( <a href="http://ldas.gsfc.nasa.gov/">http://ldas.gsfc.nasa.gov/</a> )

Monthly precipitation and maximum temperature concurrent with the fire month (PREC, TMAX) were selected as indicators of conditions for the ignition and spread of fire.

Maximum soil moisture and cumulative precipitation over the preceding year(s) (SMI12, PREC12, PREC12.6) were selected as indicators of the moisture available for the production of fine fuels that can facilitate ignition and spread in subsequent fire seasons. Westerling et al. (2003a) demonstrated the importance of a soil moisture proxy (i.e., the Palmer Drought Severity Index) derived from temperature and precipitation for concurrent and subsequent wildfire activity on a regional basis for the western United States; and Westerling et al. (2001, 2002, 2003a, b) and Preisler and Westerling (2007) have used similar variables to forecast wildfire activity on interannual to seasonal and monthly timescales.

Average spring and summer temperature (TAVG) was selected as an indicator of the timing of spring and thus the length of the dry season and, especially for higher elevation forests, the length and severity of the fire season (Westerling et al. 2006). Westerling et al. (in preparation) found the percentage of the year with snow cover is an important control on the effects of changes in the timing of spring on the length and severity of the fire season in mountain forests. Consequently, we use the interaction between spring and summer temperature (TAVG) and the average time with snow on the ground (SI) as a predictor for fire risks. It is important to note that monthly soil moisture alone may not capture the effect of a change in the timing of spring on fire risks. An early spring results in an earlier arrival of summer drought, but may not lead to large changes in soil moisture for peak summer months, when these may be typically dry anyway. Westerling et al. (2006) found that a longer dry season is associated with drier vegetation and greater fire risks in the peak summer months of the fire season in mid-elevation forests with a short snow-free season.

Long-term average soil moisture (SMI20) and elevation (ELEV) are useful indicators of the nature of the local water balance, characterizing coarse vegetation types and the likelihood that soils and fuels will dry out regularly during the summer fire season. Notice in particular the strong correspondence between coarse vegetation types and available moisture (as described by long term average precipitation and soil moisture in Fig. 2), and between available moisture and the incidence of large fires (grid cells with one or more large fires in the historical record are indicated in Fig. 2).

The factor WET was used to categorize voxels into one of two fire regimes: (1) a wet (or energy limited) fire regime, and (2) a dry (or moisture-limited) fire regime. The defining threshold for WET ( $SMI20 \geq 28\%$ ), while arbitrary, was chosen because it roughly coincided with the transition between areas where fires tend to be reported as forest fires and areas where fires tend to be reported as grass or shrubland fires within the subset of fire history data that included this information. WET serves to coarsely characterize both the vegetation type and the response of wildfire risks to climate in that vegetation type. Approximately 45% of voxels qualified as WET in the control period.

#### 4.5 Climate change simulation

The same hydrologic and climatologic variables as described above, were derived from GFDL and PCM global climate model runs for the A2 and B1 emissions scenarios. The downscaling and bias correction of the GCM precipitation and temperature follow statistical techniques originally developed by Wood et al. (2002, 2004), as described in Cayan et al. (2006). The downscaling and bias-correction methodology does not preserve the day-to-day variability from the GCM runs, with the result that changes in extremes may not be well represented. The VIC hydrologic model was run at  $1/8^\circ$  resolution over the entire domain, using the bias-corrected precipitation and temperature downscaled from the GCM runs.

#### 4.6 Statistical methodology

Because large wildfires are rare, extreme events, modeling them statistically at high resolution requires using a probabilistic risk model such as the one employed here. That is, it would be very difficult to estimate a statistical model for wildfire in each  $1/8^\circ$  grid cell by directly relating wildfire occurrences observed in that location alone to climate observed in that location alone, because over the period sampled there would be very few instances of a large fire occurring at each location. One way to get around this problem is to aggregate fire occurrence over a large area, so that in any given time period there is likely to be a fire observed somewhere within the area of aggregation. The drawback to that approach is that the results are very imprecise in terms of location, and important location-based idiosyncrasies are smeared out. This is especially a problem when trying to assess the economic impacts of changes in wildfire under climate change scenarios.

The approach explored here estimates the probability of a large wildfire in each location based on characteristics such as elevation and climate that are particular to that location, but assumes that the relationships between wildfire risks and characteristics such as elevation and climate are similar across locations ( $1/8^\circ$  grid cells) that have coarsely similar vegetation. Adopting the methodology used in Brillinger et al. (2003), Preisler et al. (2004) and Preisler and Westerling (2007), we estimate the probability of at least one large fire occurring in a voxel via a logistic regression.

Our predictand is the probability that a fire exceeds an arbitrary size threshold:

$$P_{i,j,t} = \text{Prob}[A_{i,j,t} > C | X_{i,j,t}, e]$$

where  $P_{i,j,t}$  is the probability that the voxel denoted by longitude= $i$ , latitude= $j$ , and time= $t$  contains at least one fire greater than  $C$  (where  $C=200$  ha) given a vector of predictor variables  $X_{i,j,t}$ . In this case  $X_{i,j,t}$  denotes the record of predictor variables introduced in the previous section for the voxel indexed by  $i$ ,  $j$ , and  $t$ .

Because the relationships between  $P$  and several of the predictor variables are nonlinear, a nonlinear model using basis splines was estimated using the *R* statistical package (R Development Core Team 2004). The `bs()` function in *R* was used to create basis functions for TMAX, PREC12, PREC12.6, and ELEV. The boundary knots for the PREC12, PREC12.6 and TMAX basis splines were set to limits greater than the range of variability in the climate simulations. A thin plate spline (Hastie et al. 2001; Preisler et al. 2004; Preisler and Westerling 2007) was used to estimate a two-dimensional surface describing the interaction between SI and TAVG, with the boundary knots for TAVG also set to limits greater than the range of variability in the climate simulations.

The `glm()` function in *R* was used in conjunction with the smartpred software library developed by Thomas Yee for *R* ([www.stat.auckland.ac.nz/~yee/smarter/index.shtml](http://www.stat.auckland.ac.nz/~yee/smarter/index.shtml)). Smartpred implements an algorithm devised by Chambers and Hastie (1992) to fit a generalized linear model (Dobson 1990) and to make predictions using that model, in this case on simulated climatologic and hydrologic variables.

The logistic regression model specification is:

$$\begin{aligned} \text{Logit}(P) = & A_{\text{wet}} + B_{\text{wet}} \times [X(\text{TMAX}) + X(\text{PREC12}) + X(\text{PREC12.6}) \\ & + X(\text{ELEV}) + X(\text{SI}, \text{TAVG}) + \text{PREC} + \text{SMI12} + \text{SMI20}] \end{aligned}$$

where  $P$  is the probability of a large fire event, as described above, and  $\text{Logit}(P)$  is the logarithm of the odds,  $(P/(1-P))$ ;  $X(V_i)$ wet is a matrix describing a basis spline for  $V=$

{TMAX, PREC12, PREC12.6, ELEV, SI×TAVG}; and WET={TRUE, FALSE}, and  $A$  and  $B$  are parameter vectors estimated from the data.

As a crude simplification, this model specification incorporates data that have been stratified into two simplified fire regimes: a wet, or energy-limited, regime and a dry, or moisture-limited, regime. Two models, one for wet (energy limited) and one for dry (moisture limited) settings are thus derived. All of the predictors are highly significant for both the wet and dry specifications, but the dry model is particularly sensitive to antecedent moisture, while the wet model puts greater weight on maximum temperature (TMAX) and interactions between spring temperatures and the length of time snow remains on the ground (i.e., the thin plate spline described above). This difference is consistent with the energy-limited vs moisture-limited framework described above.

Vegetation type is an important factor for characterizing both fire dynamics and hydrology. For the latter, in this analysis we were constrained to use the VIC hydrologic model with a fixed vegetation layer that did not evolve with a changing climate. In the statistical fire model specification, we use average soil moisture and snow water equivalent over the preceding 20 years for each voxel to characterize the fire regime response to temperature and to antecedent moisture. These parameters are relatively static during the reference period (1961–1990), but have the potential to vary freely as the climate simulation unfolds.

The result is that the fire risk model only partly represents potential changes in the spatial distribution of vegetation types. The spatial characterization of energy- vs moisture-limited fire regimes, used in the risk model specification as a coarse approximation of fuel types and moisture-limited vs energy-limited fire regimes, does change over time with changes in average soil moisture. However, since the hydrologic model itself is not sensitive to changes in vegetation, soil moisture changes do not reflect any feedback effects from changes in vegetation.

The estimated logistic model fits the observed data aggregated along multiple dimensions. Since the model response is a probability, it is necessary to aggregate the data in some way to facilitate comparisons with the observed data. Binning the observed large fire incidence by increments of 0.1 in the linear predictor for the logit (i.e., the right hand side of the model specification above), we see a tight fit between the estimated logit and the observations (Fig. 3a). Despite the lack of a dummy variable for month (i.e., a seasonal cycle is not directly represented in the model construction), the seasonal cycle in the estimates approximates the observed cycle (solid and dashed black lines in Fig. 3b). This result is driven purely by the seasonality that is contained in the observed climate and simulated hydrologic data that are employed in deriving the model.

The interannual variability in the observed data is also captured reasonably well by the model, as indicated by a Pearson's correlation of 0.78 between modeled and observed values (Fig. 3c). Finally, the spatial pattern of estimated fire risk (Fig. 4) is a good approximation of the spatial pattern in the observed fire risk. Given that the model specification is limited to hydro-climatic variables and elevation, the latter of which does not vary over time, the results are clear evidence that climate plays an important role in driving variability in wildfire.

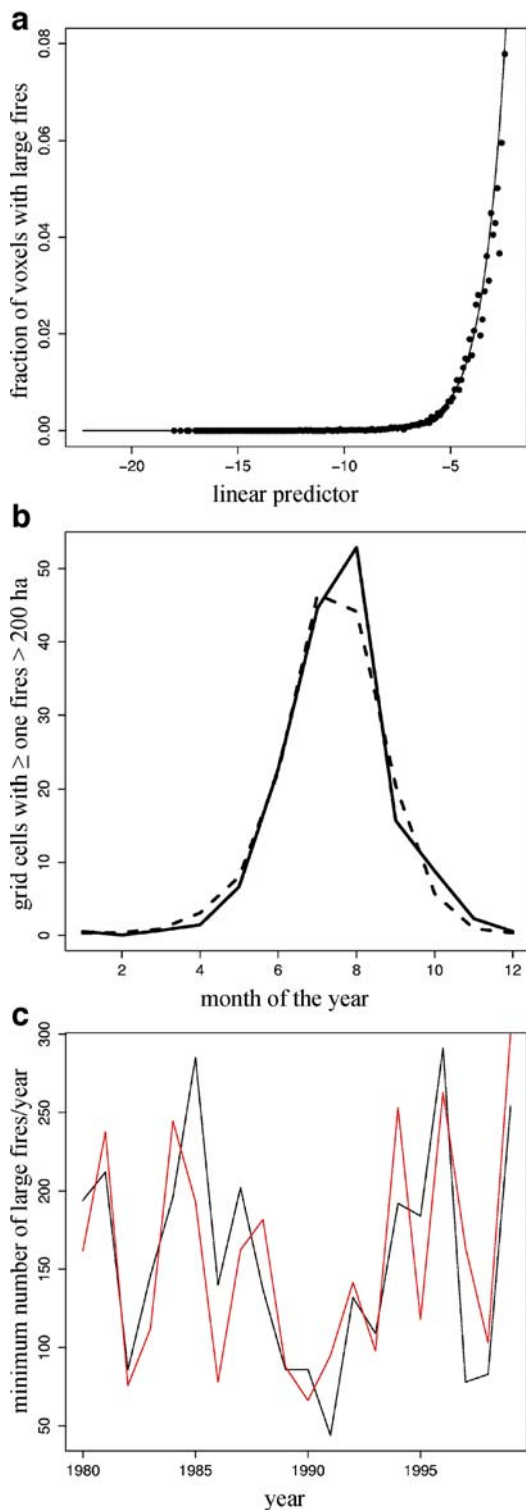
#### 4.7 Property loss modeling

In order to estimate changes in property losses associated with the climate change scenarios, property damages due to wildfires were modeled using wildfire occurrence model together with a mapping of the location and density of residential structures, which

**Fig. 3** **a** The estimated logit( $P$ ) (line), where  $P$  is the probability of observing a fire >200 ha in a voxel, vs the observed probabilities for 1980–1999 (points).

**b** Comparison of seasonal cycles for the 1980–1999 model estimation period. Fitted values (dashed) vs observed (solid).

**c** Expected voxels with fires >200 ha (red) estimated by logistic regression, by year, vs observed voxels with fires >200 ha (black), by year, 1980–1999



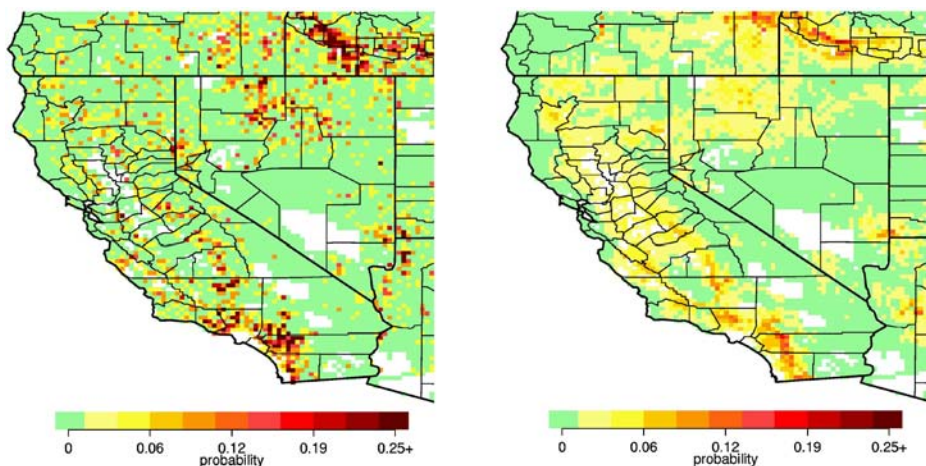


**Fig. 4** Observed (left) vs modeled (right) annualized risk of one or more fires  $>200$  ha, 1981–1999. Observed risk, based on only 20 years of records, is necessarily more “noisy” than the logistic model

was prescribed from the 2000 U.S. Census. We projected U.S. census block groups onto a finely spaced grid of over half a million points covering California. Block groups vary in area but encompass on average about 1,500 people. There are 22,133 block groups contained within California. (<http://factfinder.census.gov>) Given any set of points contained within a fire perimeter, we can use the census data and derived values to estimate total quantities of interest (e.g., number of structures, total property value) associated with those gridpoints. Lastly, to estimate damage caused by fires, we multiply the values contained within the area by empirically derived ratios for improved structure value and the number of structures destroyed, given that a fire perimeter encompassed the structures.

We extracted relevant census data from ‘Summary File 3’ for California, which is available free from the U.S. Census Bureau website. This provided information including population, number and distribution of housing units, and property value estimations for owner-occupied housing units. Estimates of both total housing structures and total property value within a census block were derived by developing weighting and scaling functions that utilize block-group-specific information on how many housing units are in structures of various sizes, combined with how many housing units were occupied by the owner, vs those that were rented or vacant. These demographic data were associated with our finely spaced grid using the Census Bureau’s census block cartographic boundary files, and scaled according to the area fraction of the block group represented by each grid point. Given a fire perimeter encompassing a set of grid points, we simply sum the values associated with those gridpoints to get an estimate of the quantities contained within that region.

Note that this approach assumes a homogeneity within block groups. However, the heterogeneity that exists should be effectively random, so that given the number of samplings used here, the effect is expected to be minimal. The homogeneity assumption may break down in extremely large block groups, but very large block groups occur when housing is very sparse, and since values are scaled down by area, the error contributed to the aggregate damage estimates should again be minimal. In general, the results should be interpreted statistically, not on a case-by-case basis.

Lastly, to estimate damages, we required a method for scaling total value enclosed to total value damaged. This is controlled by two factors: The fraction of structures damaged (given that they were encompassed by a fire perimeter), and the fraction of a property's value associated with improvements to the property (which is the fraction assumed to be lost if the home is burned). For the latter, we use estimates provided by the California Department of Forestry and Fire Protection's Fire and Resource Assessment Program (FRAP), derived from county assessor parcel data for Mariposa and Nevada counties (Robin Marose, personal communication).

To estimate the damage ratio as a function of structure density, we extracted data from archived Incident Management Situation Reports ("SIT reports") of past large fires in California (<http://iys.cidi.org/wildfire/>). These reports provided an estimate of the number of structures destroyed in each fire. We then used GIS information about the fires' boundaries to identify points on our grid contained within the fires, and used those to estimate the total number of structures contained within the fire perimeter. We then used structures contained, structures damaged, and area to generate a linear model approximating the expected value for the damage ratio, given a structure density. Note that we assume that structures termed as "lost" in the SIT reports were a total loss: we do not try to estimate the percent of a structure that is lost.

Because of the lengthy string of steps involved in creating it, the accuracy and meaningfulness of the damage ratio is likely the least certain link in the chain from data to fire estimates. In particular, the linking of fire-perimeter data with structures-damaged data was subject to substantial uncertainty due to a lack of common and unambiguous identifying information. Matching was performed only by character matching of the fire names, which were not standardized, in combination with dates. Fortunately, the effect of the damage ratio on damage estimates is effectively linear, so it is easy to note how the estimates will change, given an error in the damage ratio function.

The results of this analysis should not be particularly sensitive to either the damage ratio or the improved ratio selected. The greatest changes in losses for burned structures under the climate change scenarios were found to occur in grid cells that are very similar in terms of structure density and proximity to urban areas. Consequently, we expect them to have similar improved ratios and damage ratios. While the choice of ratios would affect the level of estimated damages in these grid points, given the similarity of the locations, it would not be expected to have a large affect on the change in damages under a climate change scenario relative to the reference period. This is in part due to the fact that we hold development fixed at the 2000 census. If we were to complicate this analysis by projecting future development scenarios, then the choices for improved ratio and damage ratio might have a greater impact on the change in damages. This would be especially true for scenarios that posited more development in mid-elevation forests that are presently sparsely populated but which account for much of the increased fire risk under the climate change scenarios considered here.

To generate the values used in this report, we approximated the effect of a 200-ha fire in each of 2,440  $1/8^\circ$  cells covering California. A 200-ha fire is represented in most cases by two gridpoints, so for each  $1/8^\circ$  cell we randomly chose two points and aggregated their values, applying the formulas described above, with some appropriate scaling to account for the discrete nature of the gridpoints. We repeat this process 100 times for each gridcell, and then retain the mean value for the number of structures at risk (i.e., contained within fire perimeters), the number of structures burned, and the value of the burned structures. To estimate the expectation for each of these values under each climate

scenario, we multiply them by the estimated probability of a large fire in each corresponding voxel.

## 5 Results and discussion

Applying the downscaled and VIC-modeled climate change projections to the fire risk model, A2 scenarios exhibited a greater increase in the probability of a large (i.e., greater than 200 ha) fire than did B1 scenarios, and GFDL a greater increase than PCM models, by mid-century (Fig. 5). Increases by 2070–2099 ranged from just over +10% to just under +40% increases overall in large fire risk over the whole region. For California only, changes by the end of the century ranged from an increase of +12% to +53% (Table 1, Fig. 5). Increases in Northern California ranged from +15% to +90%, increasing with temperature (Table 1, Fig. 6). In Southern California, the change in fire risks ranged from a decrease, −29%, to an increase, +28% (Table 1, Fig. 6), largely driven by differences in precipitation between the different scenarios. Drier conditions in southern California in both the GFDL model scenarios led to reduced fire risks in large parts of southern California, though not everywhere; for example, in parts of the San Bernardino mountains, fire risks increased.

While the higher temperatures in the GFDL model runs tended to promote fire risk overall, reductions in moisture due to lower precipitation and higher temperatures led to reduced fire risk in dry areas that appear to have moisture-limited fire regimes. The effects of lower moisture availability on fine fuel production probably outweighed the effects of temperature on fuel flammability in dry grass and shrub lands at lower elevations. This effect was particularly pronounced in much of southern California and western Arizona (Fig. 7). By contrast, the effects of temperature and lower precipitation in the GFDL runs produced larger increases in the western slopes and foothills of the Sierra Nevada and in the Coast and Cascade ranges of northern California and southern Oregon, where forests and woodlands provide a ready source of fuel (Fig. 7).

These model results indicate that scenarios that tend toward hot and dry extremes may tend to produce opposite results in moisture-limited vs energy-limited fire regimes, with

**Fig. 5** Percent change in the expected annual number of voxels (i.e., lat×lon×month) with at least one fire >200 ha for (top) region (California+neighboring states) and (bottom) California only

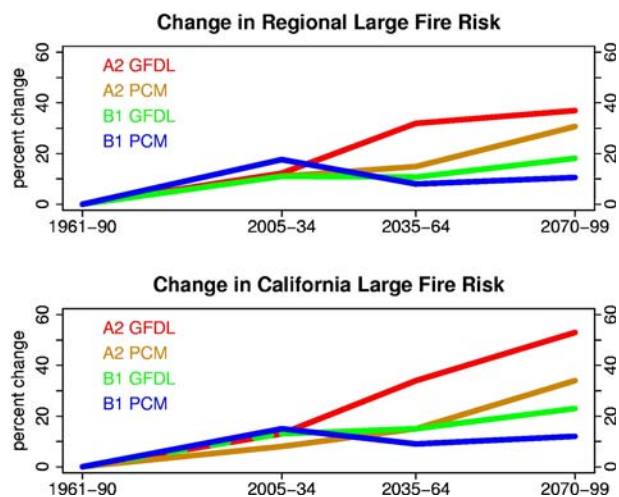


**Table 1** Percentage change in values, structures and fires, 2070–2099 over 1961–1990

	B1 PCM	B1 GFDL	A2 PCM	A2 GFDL
CA burned value	15	30	30	36
CA burned structures	6	11	21	16
CA threatened structures	7	12	21	11
CA large fires	12	23	34	53
NC burned value	21	48	37	96
NC burned structures	12	31	26	75
NC threatened structures	12	30	25	71
NC large fires	15	38	37	90
SC burned value	-6	-10	2	-3
SC burned structures	-14	-26	-9	-25
SC threatened structures	-14	-26	-9	-25
SC large fires	6	-11	28	-29

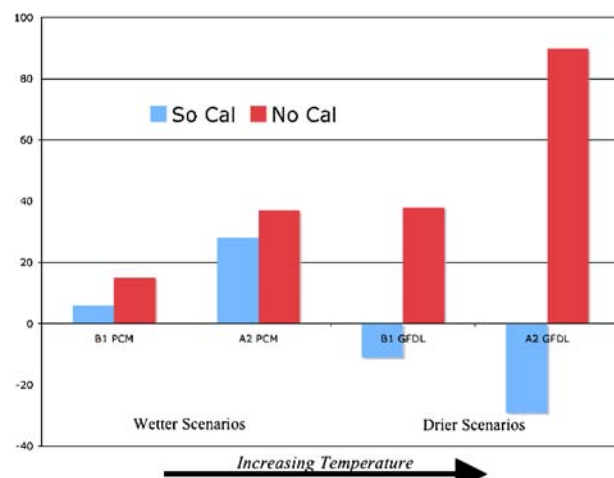
NC = Northern California, SC = Southern California

decreased fire risk over time in the former and increased risk in the latter. Conversely, wetter scenarios with more moderate temperature increases may actually result in more fire overall, as in A2 PCM vs B1 GFDL in this instance (Table 1, Fig. 7).

Comparisons across different global climate models and scenarios reveal much more uncertainty with regard to precipitation than temperature for California (Dettinger 2005). The results presented here for southern California are indicative of the effect the uncertainty regarding future precipitation has on assessing climate change impacts on moisture-limited wildfire regimes. While this uncertainty may not be reducible any time soon, a sensitivity analysis using hydrologic models and statistical fire models like those described here to determine joint temperature and precipitation thresholds for increased vs decreased fire risks in California's moisture-limited fire regimes would help to better characterize possible changes in wildfire risks for the region.

Santa Ana winds are an important component of wildfire risks in southern California that are not modeled here. To the extent that climate change could affect the frequency, strength, and/or duration of Santa Ana wind events, the results for southern California could be affected. Preliminary results of a Santa Ana wind analysis (Miller and Schlegel 2006)

**Fig. 6** Percent change in annual number of voxels (i.e., lat×lon×month) with at least one fire >200 ha for Northern and Southern California, 2070–2099 vs 1961–1990. Wetter (drier) scenarios, while still drier in Northern California, were wetter (drier) than the reference period for southern California



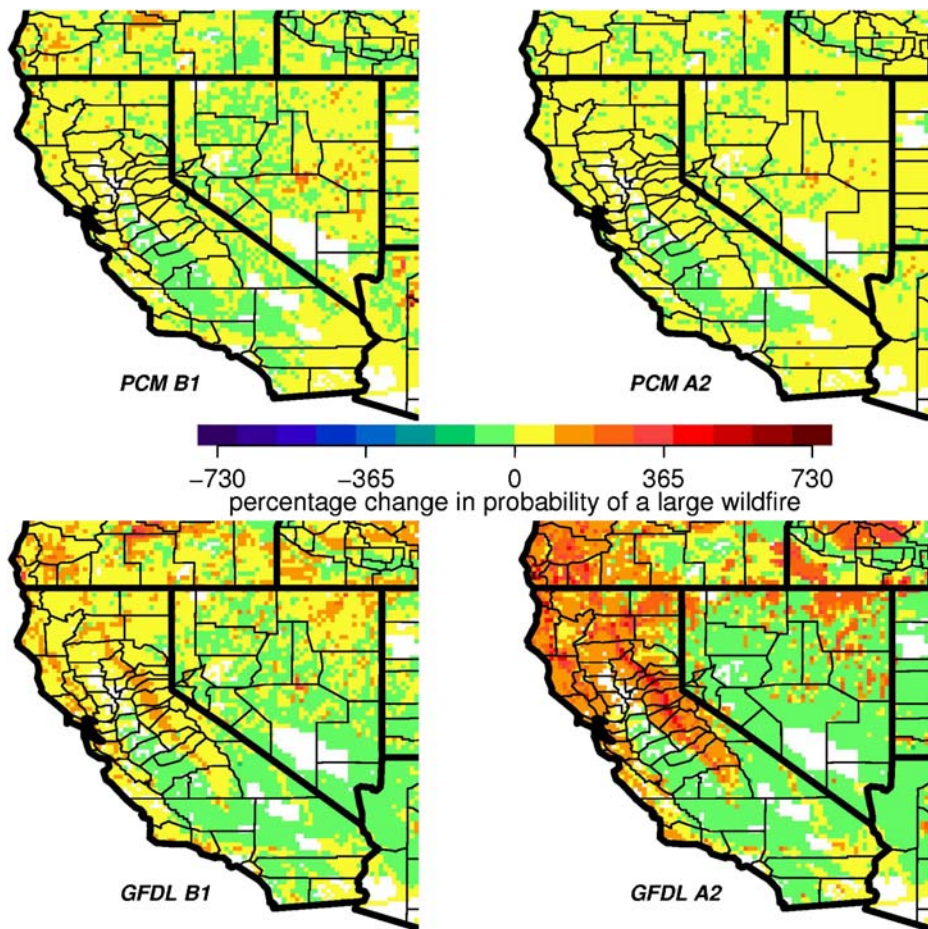


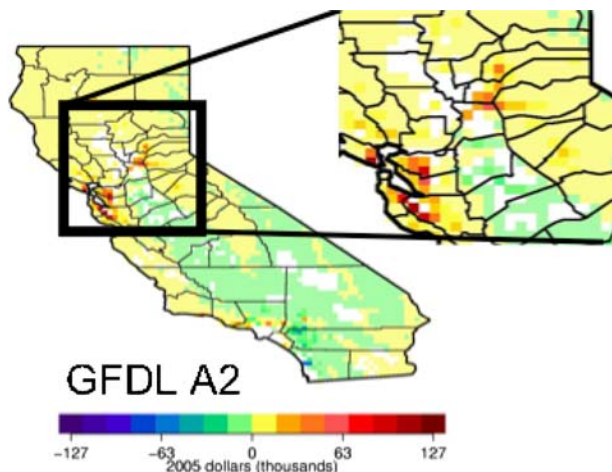
**Fig. 7** Percentage change in probability of a large wildfire by 2070–2099 over the 1961–1990 reference period for four climate scenarios

indicate, however, that the frequency of Santa Ana events in early fall, when temperatures are still high, may decrease by the end of the century, which would serve to reinforce any reductions in southern California fire risks due to changes in temperature and precipitation.

It is important to keep in mind the highly variable nature of fire risks from year to year. Scenarios with elevated fire risks on average can still produce years with very little fire, and vice versa, due to vagaries of ignitions and short term meteorology. On average, however, the results presented here indicate that increasing temperatures would likely result in a substantial increase in the risk of large wildfires in energy-limited wildfire regimes, while the effects in moisture-limited fire regimes will be sensitive to changes in both temperature and precipitation.

From the analysis of modeled property losses under the climate change scenarios, the total expected values estimated for structures burned were dominated by changes in wildfire risks proximate to a few urban areas with an extensive wildland urban interface: basically coastal counties of southern California, areas adjacent to the Bay Area, and northeast of Sacramento along Interstate Highway 80 (Fig. 8). While fire risks increase dramatically in

**Fig. 8** Difference (2070–2099 minus 1961–1990) in estimated average annual property damages due to 200 ha fires for the GFDL A2 scenario. This represents the effects of changes in the frequency of 200 ha fires



the GFDL A2 scenario in the Sierras and Coast and Cascade ranges of northern California, for example, most of these areas are relatively sparsely populated, with relatively few structures based on the 2000 census in harm's way, compared to the environs of the coastal cities. Similarly, increases or reductions in fire risks over much of the inland deserts of southern California appear to have a similarly muted effect.

Comparing Northern to Southern California based on the distribution of residential property in the 2000 census, the value of burned property in northern California nearly doubles (+96%) in the GFDL A2 scenario by the end of the century, accounting for all of the statewide increase in property damages in that scenario (Table 1). Likewise, in the scenario with the least pronounced temperature increase (PCM B1), increased damages in Northern California account for all the increase in California (Table 1).

Perhaps the most interesting result of this analysis is the effect of substantial increases in fire risks in the Sierra foothills in the GFDL A2 scenario on property damages northeast of Sacramento, particularly in Placer county (Fig. 8). Placer's population has grown at a 4% compound annual rate in the 5 years since 2000, and the county ranks among the five with the highest median incomes in California (Lofing 2006). GFDL A2 is admittedly the most extreme scenario considered here, but it is instructive in that it draws attention to developing vulnerabilities in a rapidly growing part of the state. A lesser increase in temperature and fire risk may still exacerbate vulnerabilities that may develop around future development.

However, these losses were estimated for a “fixed” landscape of residential property in California prescribed from the 2000 U.S. census. A key policy consideration for climate change impacts for wildfire in California is going to revolve around scenarios for future development. As California's population grows in the coming decades, decisions on where to locate future development will shape California's vulnerability to any climate change-induced increases in wildfire risks. In particular, development that expands the wildland/urban interface in the foothills and mountains of northern California would, based on this analysis, appear to increase vulnerability to property losses due to wildfire.

The results presented here project fire–climate relationships observed in recent decades onto twenty-first century climate scenarios. These scenarios in turn represent a range of outcomes the Intergovernmental Panel on Climate Change currently considers plausible. It is important not to over-interpret results from a statistical model of one aspect (large fire

frequency) of the complex, nonlinear, dynamic processes involved in fire ecology responses to climate change. Furthermore, climate is not the only driver of secular changes in wildfire. For example, land use and fire management will also play important roles. The reader should not place too much emphasis on the numerical levels of any of one aspect of the model's results in isolation, but instead assess the direction and degree of change in each scenario relative to the others. The model framework presented here can best be used to identify potential vulnerabilities by exploring multiple effects of climate, hydrology, and patterns of development upon wildfire.

## References

- Balling RC, Meyer GA, Wells SG (1992) Relation of surface climate and burned area in Yellowstone National Park. *Agric For Meteorol* 60:285–293
- Brillinger DR, Preisler HK, Benoit JW (2003) Risk assessment: a forest fire example. In: *Science and Statistics*, Institute of Mathematical Statistics Lecture Notes. Monograph Series
- California Board of Forestry (1995) California fire plan, pp 125
- Cayan D, Luers AL, Hanemann M, Franco G, Croes B (2006) Scenario of climate change in California: overview. California Energy Commission
- Chambers JM, Hastie TJ (eds.) (1992) Statistical models in S. Wadsworth and Brooks/Cole, Pacific Grove, CA
- Dettinger MD (2005) From climate change spaghetti to climate-change distributions for 21st Century California. *San Francisco Estuary and Watershed Science*. 3(1) Article 4. <http://repositories.cdlib.org/jmie/sfews/vol3/iss1/art4>
- Dobson AJ (1990) An introduction to generalized linear models. Chapman and Hall, London
- Donnegan JA, Veblen TT, Sibold SS (2001) Climatic and human influences on fire history in Pike National Forest, Central Colorado. *Can J For Res* 31:527–1539
- Hastie TJ, Tibshirani R, Friedman J (2001) The elements of statistical learning. data mining, inference, and prediction. Springer, New York, p 533
- Heyerdahl EK, Brubaker LB, Agee JK (2002) Annual and decadalclimate forcing of historical fire regimes in the interior PacificNorthwest, USA.. *Holocene* 12:597–604
- Houghton JT et al (Eds) (2001) IPCC climate change: the scientific basis. Cambridge University Press, Cambridge, United Kingdom and New York, NY, USA
- Liang X, Lettenmaier DP, Wood E, Burges SJ (1994) A simple hydrologically based model of land surface water and energy fluxes for general circulation models. *J Geophys Res* 99:14415–14428
- Liang X, Lettenmaier DP, Wood EF (1996) One-dimensional statistical dynamic representation of subgrid spatial variability of precipitation in the two-layer variable infiltration capacity model. *J Geophys Res* 101:21403–21422
- Lofing N (2006) Placer touts its low poverty, jobless rates. *Sacramento Bee* January 5, 2006, p. G1
- Maurer EP, Wood AW, Adam JC, Lettenmaier DP, Nijssen B (2002) A long-term hydrologically based dataset of land surface fluxes and states for the conterminous United States. *J Clim* 15:3237–3251
- Miller N, Schlegel N (2006) Climate change projected Santa Ana fire weather occurrence
- National Assessment Synthesis Team (2000) Climate change impacts on the United States: the potential consequences of climate variability and change. US GCRP, Washington DC
- NOAA (2005) <http://www.ncdc.noaa.gov/img/reports/billion/billion2005.pdf>
- Preisler HK, Westerling AL (2007) Statistical model for forecasting monthly large wildfire events in the Western United States. *J Appl Meteorol Climatol* 46(7):1020–1030
- Preisler HK, Brillinger DR, Burgan RE, Benoit JW (2004) Probability based models for estimating wildfire risk. *Int J Wildland Fire* 13:133–142
- R Development Core Team (2004) R: A language and environment for statistical computing. R Foundation for Statistical Computing, Vienna, Austria. ISBN 3-900051-07-0, URL <http://www.R-project.org>
- Running SW (2006) Is global warming causing more, larger wildfires? *Science* 313:927–928
- Sheffield J, Goteti G, Wen FH, Wood EF (2004) A simulated soil moisture based drought analysis for the United States. *J Geophys Res* 109:D24108
- Swetnam TW (1993) Fire history and climate change in giant sequoia groves. *Science* 262:885–889
- Stewart SI, Radloff VC, Hammer RB (2006) The wildland–urban interface in the United States. *Ecol Appl* 15(3):799–805

- Swetnam TW, Betancourt JL (1998) Mesoscale disturbance and ecological response to decadal climatic variability in the American Southwest. *J Climate* 11:3128–3147
- Westerling AL, Cayan DR, Gershunov A, Dettinger MD, Brown TJ (2001) Statistical forecast of the 2001 western wildfire season using principal components regression. *Experimental Long-Lead Forecast Bulletin*, 10:71–75
- Westerling AL, Gershunov A, Cayan DR, Barnett TP (2002) Long lead statistical forecasts of Western U.S. wildfire area burned. *Int J Wildland Fire* 11(3, 4):257–266
- Westerling AL, Brown TJ, Gershunov A, Cayan DR, Dettinger MD (2003a) Climate and wildfire in the Western United States. *Bull Am Meteorol Soc* 84(5):595–604
- Westerling AL, Gershunov A, Cayan DR (2003b) Statistical forecasts of the 2003 western wildfire season using canonical correlation analysis. *Experimental Long-Lead Forecast Bulletin*, 12(1, 2)
- Westerling AL, Hidalgo HG, Cayan DR, Swetnam TW (2006) Increases in Western US forest wildfire associated with warming and advances in the timing of spring. *Science* 313:940–943
- Wood AW, Maurer EP, Kumar A, Lettenmaier DP (2002) Long-range experimental hydrologic forecasting for the eastern United States. *J Geophys Res* 107:4429
- Wood AW, Leung LR, Sridhar V, Lettenmaier DP (2004) Hydrologic implications of dynamical and statistical approaches to downscaling climate model outputs. *Clim Change* 62:189–216